HIPPOCAMPUS 22:604–618 (2012)

Head Direction Cells in the Postsubiculum Do Not Show Replay of Prior Waking Sequences During Sleep

Mark P. Brandon,* Andrew R. Bogaard, Chris M. Andrews, and Michael E. Hasselmo*

ABSTRACT: During slow-wave sleep (SWS) and rapid eye movement (REM) sleep, hippocampal place cells in the rat show replay of sequences previously observed during waking. We tested the hypothesis from computational modeling that the temporal structure of REM sleep replay could arise from an interplay of place cells with head direction cells in the postsubiculum. Physiological single-unit recording was performed simultaneously from five or more head direction or place by head direction cells in the postsubiculum during running on a circular track allowing sampling of a full range of head directions, and during sleep periods before and after running on the circular track. Data analysis compared the spiking activity during individual REM periods with waking as in previous analysis procedures for REM sleep. We also used a new procedure comparing groups of similar runs during waking with REM sleep periods. There was no consistent evidence for a statistically significant correlation of the temporal structure of spiking during REM sleep with spiking during waking running periods. Thus, the spiking activity of head direction cells during REM sleep does not show replay of head direction cell activity occurring during a previous waking period of running on the task. In addition, we compared the spiking of postsubiculum neurons during hippocampal sharp wave ripple events. We show that head direction cells are not activated during sharp wave ripples, whereas neurons responsive to place in the postsubiculum show reliable spiking at ripple events. © 2011 Wiley Periodicals, Inc.

KEY WORDS: head direction cells; postsubiculum; sleep replay; retrieval; rapid-eye-movement sleep; medial temporal lobe; local field potential

INTRODUCTION

Lesion studies have highlighted the role of the postsubiculum, medial entorhinal cortex, and hippocampus in spatial memory function. For example, in the Morris water maze impairments are observed following selective lesions of the hippocampus (Morris et al., 1982), dorsolateral band of the entorhinal cortex (Steffenach et al., 2005), and the postsubiculum (dorsal presubiculum; Taube et al., 1992). Neural activity in these structures shows properties appropriate for encoding and retrieval of spatial information. Postsubiculum neurons are tuned to cardinal head direction (Taube et al., 1990a; Sharp, 1996; Goodridge and Taube, 1997; Taube and Bassett, 2003; Cacucci et al., 2004). Largely sensory driven, these head direction cells receive visual and vestibular input to keep track of head direction (Taube et al., 1990b; Goodridge and Taube, 1997; Taube and Bassett, 2003), and in some cases can code for the speed of translational motion (Sharp, 1996; Goodridge and Taube, 1997; Sharp et al., 2001). The postsubiculum provides input to the medial entorhinal cortex (Witter et al., 2000), where grid cells have been demonstrated (Hafting et al., 2005; Moser and Moser, 2008). Grid cells may project to the hippocampus, where recordings show place cells that code discrete locations (O'Keefe and Dostrovsky, 1971; McNaughton et al., 1983; Muller et al., 1987; Wood et al., 2000).

Replay of neural activity during waking and sleep has been proposed as a mechanism for consolidation of previously encoded information (Buzsaki, 1989; Wilson and McNaughton, 1994; McClelland et al., 1995; Hasselmo et al., 1996). Neurophysiological recordings in hippocampal region CA1 demonstrate that the spiking activity associated with a sequence of locations is replayed during slow-wave sleep (SWS; Skaggs and McNaughton, 1996; Lee and Wilson, 2002), during rapid eye movement (REM) sleep (Louie and Wilson, 2001) and during waking (Foster and Wilson, 2006; Diba and Buzsaki, 2007; Davidson et al., 2009; Karlsson and Frank, 2009). Data shows that hippocampal ensembles replay at two speeds. During sharp-wave-ripples in SWS hippocampal ensembles reactivate at speeds $\sim$20 times faster than stimulus presentation (Skaggs and McNaughton, 1996; Lee and Wilson, 2002; Diba and Buzsaki, 2007). During REM sleep, hippocampal ensembles replay much slower, at speeds comparable to stimulus presentation (Louie and Wilson, 2001).

During waking behavior, combined recordings of both head direction cells and place cells show that they rotate together when visual cues are rotated (Knierim et al., 1995) suggesting that they function together as a coherent spatial representation. Therefore, it seems plausible that head direction cells should show replay together with hippocampal place cells, but tests of head direction replay have not been published. Previous studies have shown that hippocampal ripples trigger spiking and replay in distant brain

Department of Psychology and Program in Neuroscience, Center for Memory and Brain, Boston University, Boston, Massachusetts
Grant sponsor: NIMH Silvio O. Conte Center; Grant numbers: NIMH MH71702; NIMH R01 MH60013; Grant sponsor: NSF Science of Learning Center CELEST; Grant number: SBE 0354378; Grant sponsor: Office of Naval Research; Grant number: NIMH R01 MH61492.
*Correspondence to: Mark P. Brandon and Michael E. Hasselmo, Department of Psychology and Program in Neuroscience, Center for Memory and Brain, Boston University, 2 Cummington St., Boston, MA 02215.
E-mail: markpb68@gmail.com, hasselmo@bu.edu
Accepted for publication 30 November 2010
DOI 10.1002/hipo.20924
Published online 20 April 2011 in Wiley Online Library (wileyonlinelibrary.com).

structures with a wide functionality, including the primary visual cortex (Ji and Wilson, 2007), ventral striatum (Pennartz et al., 2004), and prefrontal cortex (Euston et al., 2007). However, REM replay has not been observed outside of the hippocampus. Here, we present data testing the hypothesis that replay of episodes during SWS and REM sleep may use a circuit including head direction cells (Hasselmo, 2008b; Hasselmo and Brandon, 2008). The computational validity of this hypothesis was already tested in simulations showing that REM replay could involve a circuit of place cells driving head direction cells to update grid cell representations that update place cells (Hasselmo, 2008b; Hasselmo and Brandon, 2008).

We tested the hypothesis in the experiments presented here by collecting in vivo spiking data from postsubicular head direction cell ensembles during waking and sleep. By using both a template matching correlation analysis and Bayesian decoding of head direction we show that head direction ensembles do not exhibit significant replay during REM sleep or SWS. We explore head direction cell activity during REM sleep and SWS and discuss implications of these results for current models of hippocampal circuit retrieval.

METHODS

Subjects and Pretraining

Successful recordings of the simultaneous activity of multiple neurons in the postsubiculum were obtained from three male Long Evans rats (500–600 g). All experimental procedures were approved by the Institutional Animal Care and Use Committee for the Charles River Campus at Boston University. Rats were individually housed in plexiglass cages, maintained on 24/h light/dark cycle (testing always occurred during the light cycle) and were maintained at ~85% of their ad libitum weight. Before surgery, animals were habituated to experimenter interaction and the testing room. To obtain consistent sequential activation of head direction cells during waking, animals were trained to run clockwise on a circle track for food reinforcement (1/4 froot loops), fixed at the northernmost location on the track. The circle track had a track width of 9 cm, a diameter of 109 cm, and a circumference of 342.4 cm. An array of complex visual cues was placed on the walls of the recording room to provide stable landmark information. A revolving boom rose from the center of the circular track intended to later support the weight of the tether and head stage above the animals' heads during recording sessions. Pre-surgical training was complete once animals could complete 25 laps of the track within 15 min.

Surgery

All surgical procedures followed National Institute of Health guidelines and the protocol approved by the Boston University Institutional Animal Care and Use Committee. Each rat was given Atropine (0.04 ml/kg) 20 min prior to initiation of Isoflurine-induced anesthesia. Animals were maintained for the duration of surgery with a combination of Isoflurane and a Ketamine cocktail (Ketamine 12.92 mg/ml, Acepromazine 0.1 mg/ml, Xylazine 1.31 mg/ml). Following placement in a stereotaxic holder, skin and epithelium were cleared from the skull and anchor screws were inserted along the periphery of the dorsal surface of the skull. One anchor screw, positioned anterior to bregma, was wired to the implant and used as a recording ground. Craniotomies were made above the left hippocampus (ML −2.0, AP −3.5) and the right postsubiculum (ML −3.2, AP −7.2) and the dura mater was removed. Theta was consistently detected in the postsubiculum; however, we also chose to insert an additional bundle of electrodes into the hippocampus for two of our three animals to acquire a more robust theta signal. A group of four EEG electrodes (40 μ, California Fine Wire Company) were lowered 2.0 mm below the dorsal surface into the hippocampus. In all animals, a bundle of 11 recording Tetrodes (four 12.7 μ diameter wires twisted together, Kanthal) were placed on the dorsal surface of the brain just above the postsubiculum. Before surgery, tetrode tips were gold plated to reduce the impedance to ~250 kΩ. Immediately following surgery, all tetrodes were lowered 1 mm ventral to the dorsal surface. After surgery, animals were allowed to recover for 7 days before further testing.

Neural Recordings

Tetrodes were gradually lowered into the postsubiculum over the course of 7–10 days guided by stereotaxic atlas depth coordinates (The Rat Brain Atlas, 4th Edition), local field potentials, theta rhythmic units, and head direction selective units. Neural signals were preamplified by unity-gain operational amplifiers located on the head stage (Neuralynx, Tucson, AZ) of the animal. Signals were then amplified (5,000–20,000×) and bandpass filtered (0.3–6 kHz; Neuralynx, Tucson, AZ). When a signal crossed threshold all four channels of the tetrode were digitized at 32 kHz and recorded (Neuralynx). Position and head direction data were calculated using an asymmetric linear display of light-emitting diodes located on the head stage of the animal during recording. Head direction was determined by tracking the most caudal and most rostral LED and calculating the angle between their positions. Intermittent flips of 180°, which lasted for less than five tracking samples (166 ms) were replaced by a linear interpolation between the sample before and the sample after the flip. Position was determined as the centroid of all diodes.

Generally, tetrodes were adjusted days before recordings would begin, and tetrodes were not moved for at least an hour before recording to promote stability. Neural activity was recorded during a 90–120 min sleep pre-task session on a pedestal located adjacent to the circle track. Following the sleep session, while remaining on the pedestal, animals were passively rotated for ~5 min to sample all head directions. Animals were then given access to a bridge that led them onto the circle track. As initially trained, animals would then run clockwise on the circle track for food reinforcement (1/4 froot loops), fixed at the northernmost location on the track. This running pattern ensured that rats would experience consistent sequential sampling of a full cycle of head direction angles to provide sequential activation of head direction cells during waking. After ~25 complete laps on the track, animals returned to the sleep pedestal for a second 90–120 min sleep session.

Spike Sorting

Single-units were isolated "offline" manually using graphical cluster cutting software (Offline Sorter, Plexon). Neurons were separated based on the peak amplitude, energy, and the first principal components of spike waveforms (Offline Sorter, Plexon). Evaluation of the presence of biologically realistic inter-spike intervals, temporal autocorrelations, and cross correlations was used to confirm single unit isolation.

REM Detection

Local field potential (LFP) traces obtained from the CA1 region of the hippocampus were used to detect periods of network oscillations during sleep consistent with REM sleep. Field potential traces were bandpass filtered to delta (2–4 Hz) and theta (6–10 Hz) ranges. The filtered delta and theta LFP were divided into 1 s bins. For each bin, the delta and theta powers were computed as the time-averaged squared amplitude of the filtered trace (Louie and Wilson, 2001). Bins with a theta to delta power ratio of >2.0 were considered to be periods of high theta activity. As in previous studies (Louie and Wilson, 2001), REM epochs were defined as periods of high theta activity with duration >30 s with lack of movement as determined by a kalman filter velocity estimation threshold of 1.5 cm/s.

Ripple Detection

Field potential data was also analyzed to detect ripple/sharp wave events during SWS and quiet waking, because previous studies show that replay during SWS occurs during hippocampal ripples. Hippocampal CA1 local field potential epochs containing high theta power (theta to delta ratio >2.0) were excluded from ripple detection to prevent false-positive identifications during high frequency events during theta. Non-theta traces were bandpass filtered between 80 and 250 Hz. We defined the detection signal as the ripple envelope as described in (Nguyen et al., 2009). Briefly, the ripple envelope is defined as the instantaneous signal amplitude, calculated from the magnitude of the Hilbert transform of the filtered signal, and then smoothed by convolution with a Gaussian kernel with a standard deviation of 50 ms. Putative ripple event centers were defined as the maximum value during deviations in detection signal greater than three standard deviations above the mean. Ripple onset and offset were defined by detection signal deviations greater than 1.5 standard deviations above the mean (Nguyen et al., 2009). Events <20 ms in duration were excluded, and there was no maximum duration. Infrequently, epochs of sustained high frequency activity were detected up to 1.62 s in duration, and were most likely caused by multiple consecutive ripple events.

Cell Selection

Cells were classified as head direction cells or place responsive cells using the following method. Head direction cells were defined as neurons that contained both a localized firing field on the circle track and a corresponding directional field on the adjacent pedestal. Place responsive cells were defined as neurons with a place field on the circle track but no directional preference on the pedestal. The mean direction was defined as the direction of the resultant vector of the directional firing rate distribution:

$$\bar{\theta} = \arctan\left(\frac{\sum_{i=1}^{n} F_i \sin(\theta_i)}{\sum_{i=1}^{n} F_i \cos(\theta_i)}\right),$$

where i is the bin index, n is the number of bins (60), F_i is the frequency in bin i, and θ_i is the direction of bin i. The mean resultant length, R was defined as

$$\bar{R} = \frac{\cos(\bar{\theta})\sum_{i=1}^{n} F_i \cos(\theta_i) + \sin(\bar{\theta})\sum_{i=1}^{n} F_i \sin(\theta_i)}{\sum_{i=1}^{n} F_i}.$$

The circular variance (S) is defined as $S = 1 - \bar{R}$. S ranges from 0 to 1, inclusive, which is different from the variance of non-directional data. The circular variance is a convenient measure of the spread of directional data. A dense bundle of vectors will yield an R value closer to 1, so the variance will be low. All cells with a maximum firing rate >2 Hz on the circular track were candidate head direction or place responsive cells. Head direction cells were those whose firing frequency directional variance on both the circular track and pedestal were <0.8, and whose difference in mean direction between the circular track and pedestal was <90°. Cells with variance <0.8 on the circular track, but >0.8 or with a maximum firing frequency on the pedestal <1 Hz were classified as place responsive cells. For place responsive cells, maximum directional firing frequency on the pedestal could not exceed half the maximum firing frequency on the circular track. Spikes for all cells were visually inspected to include those with orientation tuning (fields 180° apart), or those with multiple tuning fields. Cells that either ceased or began firing during the recording session were assumed to be a result of tetrode drift and were excluded from our analysis.

Correlation Analysis

To explore the potential for multi-unit replay activity during REM sleep, we replicated a template matching analysis described in Louie and Wilson (2001). For each recording session, each REM window was compared with the waking period by sliding the REM window across the waking period and calculating a normalized correlation at each time point, using the procedures described here. For neuronal activity on each day during the full period of the running task (RUN) and each epoch of REM sleep (REM), the spike data was transformed into a $C \times N$ spike activity matrix, where C is the number of directionally sensitive cells from the recording session and N is the length of the epoch in 1 s bins. Each matrix was smoothed in time by convolution with a Gaussian of standard deviation 1.5 s. A time-varying correlation coefficient, Ct, was calculated between each REM epoch template matrix and the full RUN matrix.

To account for differences in temporal scaling, a scaling factor (SF) determined the size of the window of RUN activity compared with the template. SF ranged from 0.3 to 3.0 and the window of RUN was calculated as the duration of the REM template divided by SF. Thus, no change in RUN (waking) corresponded to scaling factor = 1.0, whereas compression of the waking period corresponded to smaller scaling factors, and expansion to larger scaling factors. In other words, values of SF <1 indicate REM replay faster than the RUN activity, and values of SF >1 indicate REM replay slower than the RUN activity. Each REM template was slid across RUN activity to produce a matrix of correlation scores varying in time and scaling factor, Ct(t, SF).

As done previously (Louie and Wilson, 2001), we performed a data bootstrap to test the statistical significance of the Ct values. In this bootstrap procedure, the correlation to the actual REM template spiking activity was contrasted with the correlation to template activity that had been shuffled in multiple different permutations. For each Ct(t, SF), four sample distributions resulting from unique shuffling algorithms were produced. The data was shuffled prior to Gaussian smoothing in the following ways. In the first type of shuffling, the time bins for each cell were randomly permutated to remove the temporal alignment for each cell individually. For the second type of shuffling, the time bins were again randomly permutated, but the temporal alignment across cells was preserved. For the third type of shuffling, the cells were randomly permutated while the temporal order of spike activity within each spike train was preserved. For the final type of shuffling, each cell's entire spike train was temporally shifted relative to the original alignment while preserving relative temporal order. This shift was circular so that the data removed from one end was reinserted at the opposite end. Fifty shuffled templates were generated for each method.

Once the four shuffled distributions of Ct values were generated, the significance of the original Ct was compared to each distribution to calculate Z score values. The least significant of the resulting four Z score values was assigned to the time index and scaling factor of the corresponding Ct value. This resulted in a two-dimensional array of Z scores corresponding to each time bin of the RUN template and scaling factor. To then gauge the correlation of the REM epoch with the entire RUN data set, the RUN data was parsed into laps and they were aligned behaviorally by aligning the times of peak displacement of the rat along the x dimension in space (halfway through the lap). The aligned Z scores were then averaged and the peak value was used to assess the significance of the correlation and indicate the scaling factor for which the correlation of REM data with RUN data was maximum.

Modified Template Correlation Analysis

In addition to the analysis presented above, we also modified the Louie and Wilson analysis to explore the effect of lap alignment and averaging. In the final step of the original analysis above, all laps were behaviorally aligned and averaged, yet the longer laps on the full circular track could result in variability in RUN activity that might render averaging uninformative. To account for this, we changed the template used for correlation analysis. Instead of using the spiking activity during a REM epoch, we used the spiking activity during individual laps of running. Thus, each individual lap (RUN template) was compared to entire REM epochs. In this case, the template duration was not divided by the scaling factor, but rather multiplied by the scaling factor to determine the size of the window of REM activity compared at each SF. This way, the convention SF >1 denoting slow replay was conserved. Figures 4A and 4B shows the resulting matrices of Z scores from six RUN template to a particular REM epoch.

To test which lap analysis should be averaged, we calculated Ct scores pairwise for each lap relative to each other lap to center the laps on one another. We noted laps that were statistically similar, and those that were not, from the same session. This was often due to differences in lap duration. The mean lap duration was 7.52 s, with a standard deviation of 1.43 s, and a mean number of 21.25 laps in each session. There were 85 total laps across sessions. Within a given session, there were laps that the animal ran slowly (about 10 s), and laps that the animal ran quickly (about 5 s). In two sessions it was clear that the animal was exhibiting two distinct behaviors on the track, and there was a bimodal distribution of lap duration. Every animal showed a range of lap duration from 5 to 11 s. We used a clustering algorithm (complete linkage, Statistics Toolbox, MATLAB2007B) to group together only laps that were statistically similar via the same bootstrapping analysis, and averaged analyses within the groups (N = 15 groups). There were about 3.75 groups within each session, and the maximum observed cluster size was 10 laps. Only groups with three or more laps were considered. Figures 4A and 4B shows how the selective averaging retains peaks relevant to different lap template activity. Those differences are shown in Figure 4C, where the raster plot shows different firing of multiple head direction cells during the same recording session. Furthermore, this switch in template definition simplifies averaging since the underlying duration of REM activity does not change, there is no need for alignment. Despite careful separation of distinct template activity to prevent loss of significant Z scores, the number of significant Z scores does not change much from the original analysis, as shown in Figure 4D.

Bayesian Head Direction Reconstruction

To visualize encoding of head direction in ensemble activity, we reconstructed head direction using a basic Bayesian reconstruction (Zhang et al., 1998; Johnson et al., 2005). Reconstructing head direction without a continuity constraint allowed us to explore the possibility of trajectory replay during REM and SWS. First, we estimated tuning curves for each head direction-responsive and place-responsive cell in the ensemble for at least half of the time while the animal was running on the circular track. Spike head direction information was binned (width = 10°) and the resulting histogram was normalized by occupancy in each head direction bin. Using a sliding window (width = 500 ms, step-size = 100 ms), we stepped through epochs for which we want to reconstruct head direction and calculated the conditional probability $P(\mathbf{r}|\mathbf{n})$ of head direction, $\mathbf{r}$, given the ensemble firing rates, $\mathbf{n}$, for each window of activity centered on the time point for which we were performing reconstruction. Figure 5A shows the reconstruction of head direction during a period of 2 min of time on the circular track that was not in the data used to generate the tuning curves for the statistical model. Most probable head direction max$[P(\mathbf{r}|\mathbf{n})]$ is indicated by the blue dots, while observed head direction is shown by a red line. Figures 5B,C show reconstruction during REM and SWS in the same session.

Histology

Tetrodes were not moved after the final recording session. Animals were overdosed with Isoflurane and were perfused intracardially with saline and then 4% formaldehyde. Brains were removed and were stored in 4% formaldehyde at 6°C for up to 1 month. Brains were transferred into a 30% sucrose solution for up to 1 week before it was frozen in a cryostat where 40 μ thick slices were taken either on a coronal or a sagittal plane. Brain sections were mounted on glass slides and stained with neutral red Nissl stain. Tetrode tracks were confirmed to be localized within the postsubiculum and EEG electrode tracks were localized within the CA1 region of the dorsal left hippocampus. A few tetrode tracks were located in the subiculum near the border of the postsubiculum.

RESULTS

Head direction and place cell ensembles from the postsubiculum were collected from three animals during extended sleep sessions before and after behavior on a circle track, and compared with activity during running on the circle track. The anatomical location of tetrode tracks in the postsubiculum and electrode tracks in the hippocampus were confirmed with histology that is shown in Figure 1.

A raster example of a postsubiculum ensemble is shown in Figure 2A. This plot shows the spiking of eight different individual neurons when the rat was at different locations on the circular track linearized on the x axis. For each neuron, the spiking during all trials is grouped together on the y axis. This shows the consistency of neuron firing at individual locations corresponding to individual head direction angles experienced along the circular track.

Two types of cells that have been characterized in the postsubiculum are head direction cells (Taube et al., 1990a) and place by head direction cells (Caccuci et al., 2004). Since head direction cells will appear to have a "place field" on a circular track, we recorded all cells in two of our animals on a pedestal adjacent to the circle track. Cells with similar tuning to head direction on the circular track and on the pedestal were classified as head direction responsive neurons. The left column of Figure 2B shows examples of head direction responsive cells, demonstrating their similar response on the circular track and the pedestal. In contrast, cells with no activity on the pedestal and a place field on the track, or cells with dissimilar tuning between the pedestal and track were classified as place responsive cells. The right column of Figure 2B shows examples of place responsive neurons that show selective firing on the circular track, but do not show differential firing on the pedestal. Overall, there were 29 head direction responsive cells and eight place responsive cells collected across sessions. With these two behavioral tests, it was not possible to differentiate between place and place by head direction cells. Testing for pure place responsiveness would have required running the rats on an open field each day, which would have disrupted the regularity of spatial experience and interfered with testing for replay.

We calculated the mean firing rate and coefficient of variation of recorded cells during the running task, SWS, REM, and ripple epochs. Note that ripple events include ripples during both waking and SWS, and the waking and SWS epochs exclude ripple events. The mean firing rate was calculated by the total number of spikes during a given epoch over the total duration of those epochs. The CV was calculated as the standard deviation of the set of ISIs from a given epoch type over the mean. The mean firing rate of neurons responsive to place was similar to neurons responsive to head direction during the task (Place: 3.9 ± 1.79 Hz vs. Head Direction: 2.7 ± 0.51 Hz), similar during SWS epochs (Place: 1.9 ± 0.60 Hz vs. Head direction: 2.1 ± 0.40 Hz), similar during REM epochs (Place: 2.4 ± 0.94 Hz vs. Head direction: 3.1 ± 0.58 Hz), and showed the most significant difference during ripple events, when place cells fired faster than head direction cells (Place: 4.2 ± 0.75 Hz vs. Head direction: 2.9 ± 0.54 Hz; $P = 0.26$, two-sample t test). The coefficient of variation showed similar trends between both cell types (task: place = 2.57 ± 0.37, hd = 2.44 ± 0.18; SWS: place = 2.08 ± 0.11; hd = 2.27 ± 0.15; REM: place = 2.32 ± 0.13; hd = 2.69 ± 0.26). CV is not reported during ripple events because the epoch duration was often very short and therefore led to artificially stereotyped ISIs.

We compared the population of individual head direction cell statistics between different epochs using paired t tests and did the same for the population of place cell statistics between different epochs. The paired t test was not significant except for the following comparisons. The population of place cells fired significantly faster during ripple events than during SWS (ripples: 4.2 vs. SWS: 1.9 Hz; $P < 0.001$). The population of head direction cells fired slightly faster during ripples than SWS (ripples: 2.9 vs. SWS: 2.1 Hz, $P < 0.001$), and slightly faster during REM than SWS (REM: 3.1 vs. SWS: 2.1 Hz; $P < 0.001$). The

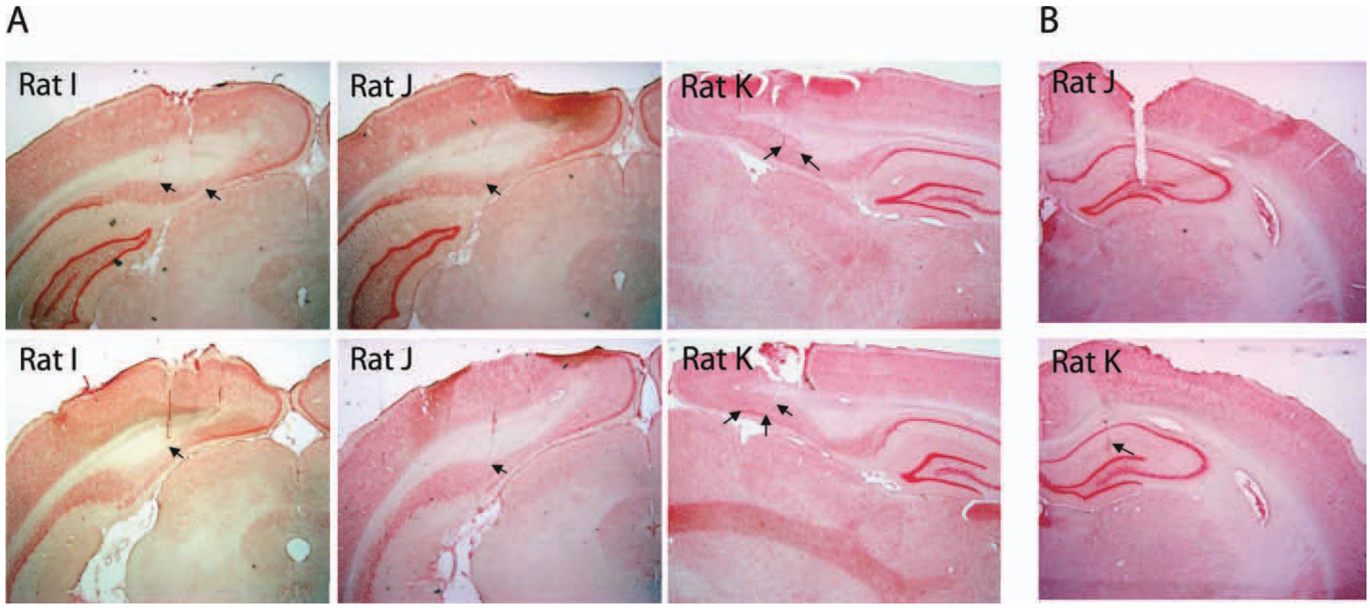

FIGURE 1. Histology. Coronal and sagittal sections were prepared with Neutral Red Nissl stain to visualize tetrode and electrode tracks. A: The tracks of tetrodes were located in the postsubiculum for all three rats, as indicated by arrows. B: Electrodes were confirmed to be localized in the hippocampus for rats J and K. Rat I was not implanted with hippocampal electrodes. [Color figure can be viewed in the online issue, which is available at wileyonlinelibrary.com.]

coefficient of variation in head direction cells was higher during REM than SWS (REM: 2.69 vs. SWS: 2.27; $P < 0.05$).

In addition, we calculated cross correlations between the spike trains of pairs of head direction cells during the task, SWS, REM, and ripples. Cells with head direction specificity during the task showed a bump in the correlation during task at lags consistent with spacing between the fields on the circular track. No head direction cell pairs that showed this correlation during the task had peaks in the REM or ripple cross correlations. A small number (<10%) of head direction cell pairs (5 of 56) showed a bump for small time lags (<100 ms) during SWS (that is, during SWS epochs outside of ripple events).

The template matching analysis, developed by Louie and Wilson (2001) was applied to simultaneously recorded ensembles of both head direction responsive cells and place responsive cells to compare the temporal structure of spiking activity during running on the circle task with the temporal structure of spiking activity in the same ensemble of neurons during REM sleep on the same day. The mean ensemble size was 6.4 neurons (minimum = 5 neurons, maximum = 8 neurons). The result of the correlation analysis for an example ensemble of neurons is shown in Figure 3A. The colors in the Figure show the significance of the correlation of a single REM epoch with different time periods of spiking activity during running on the behavioral track (x axis) and with different scaling factors (y axis). Visual inspection reveals what appears to be an increase in correlation of the REM epoch spiking activity with spiking activity at each lap on the track (Fig. 3A). However, when laps were averaged, the peak correlations values were not significantly different than our shuffled surrogate data, signified by peak Z score values of <2.0 (see Fig. 3B—peak Z score 1.6). Figure 3B shows the lap averaged Z score values for the example shown in Figure 3A, illustrating the low value of the averaged Z score. The peak Z score from this plot and other lap averaged data was used to create the histogram in Figure 3C, that shows all template results from six ensembles of neurons tested over 45 REM epochs. Almost all lap-averaged peak Z scores fell below a 2.0 criteria for significance (the significance at $P < 0.05$ is only achieved when the Z score is >2.0). Thus, using the same analysis as Louie and Wilson (2001) for postsubiculum populations we show that these ensembles are not showing temporally structured replay during periods of REM sleep.

We applied a modified template matching analysis to determine whether variability in behavior between individual laps run on the circle track could explain our less than significant correlations when laps were averaged. Figure 4A left shows the Z score results of three similar running laps compared to a single REM epoch from the same day. Figure 4A right shows the average of those correlations. For comparison, Figure 4B left shows the Z score results of a different set of three running laps from the same recording session compared to the same single REM epoch as Figure 4A left. Figure 4B right shows the average of this different group of correlations. Notice the similarity of Z score values within each lap group and the dissimilarity between the two lap groups. As shown in Figure 4C, the difference between these laps is easily seen in ensemble rasters centered at the middle of each lap. The difference in neural activity could be explained by variability seen in the passage through place fields (Fenton et al., 1998) or possibly by subtle changes in head orientation. This analysis grouped the lap runs according to their similarity in behavior, however, when similar lap groups were used to calculate peak Z scores we still did not see significant

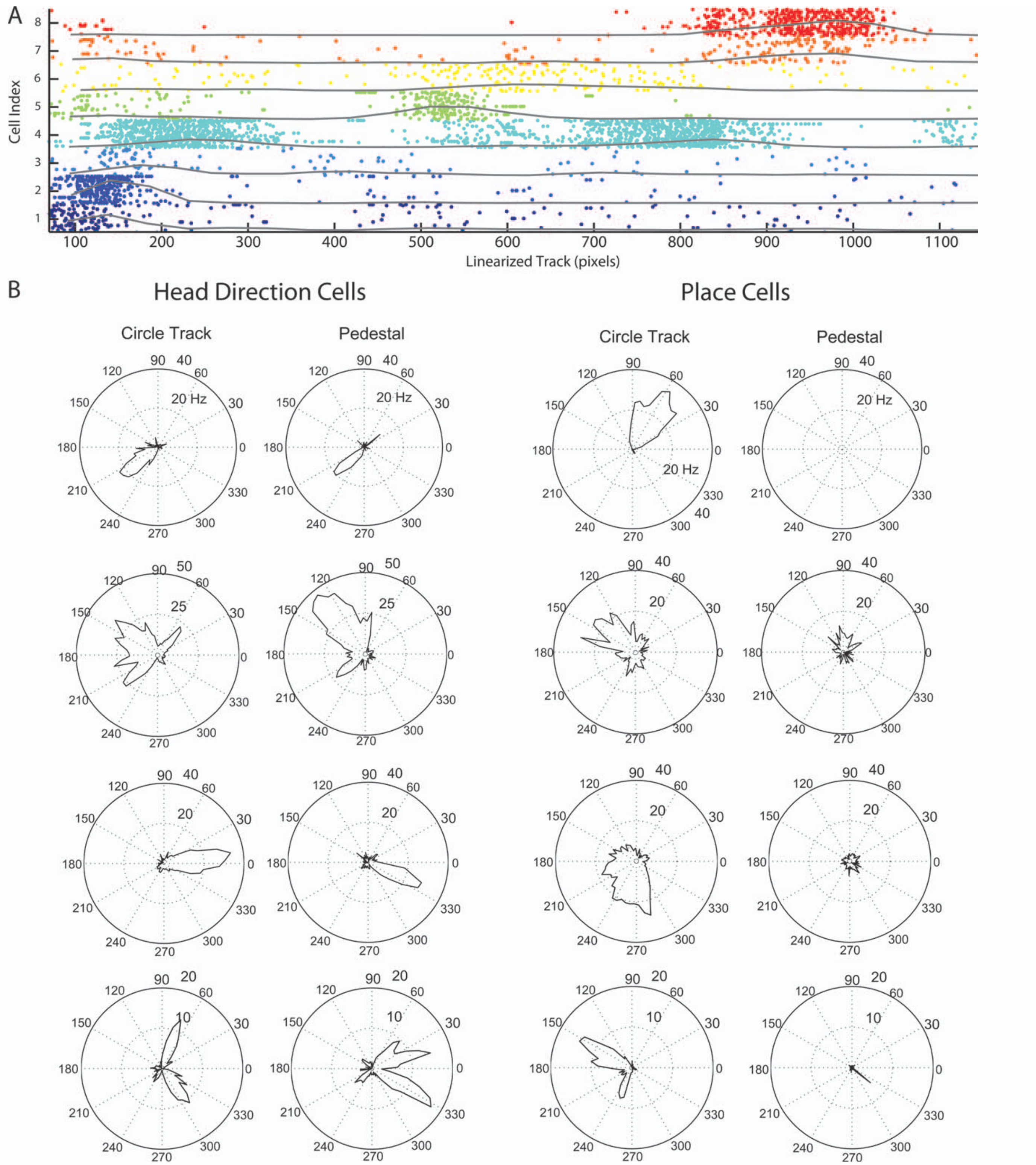

FIGURE 2. Raster plot of simultaneously recorded cells with example polar rate maps. A: Eight different head direction cells are plotted, each with a unique color. Every dot indicates an action potential. The *y* axis shows the cell index of each neuron, with laps plotted in order of performance for each neuron. The *x* axis is the linearized location on the circular track, which directly corresponds to head direction during behavior. Note that many cells show selective firing on one segment of the track, whereas cell 4 exhibits tuning to more than one direction. The frequency envelope shown as a gray line for each neuron was calculated by binning spikes at a relevant spatial bin size (50 pixels), and then smoothing with a two-bin width sliding window average. Peaks in the frequency envelope yield a sequence of head direction cell firing so that we could explore ripple replay. B: Examples of polar plots showing firing rate (dotted circles) relative to head direction angle for individual neurons. (No correspondence with A.) Head direction: Four examples of cells showing firing dependent on head direction angle on both the circle track and the rotating pedestal. There were 7 of 29 head direction cells with bimodal tuning curves. Place: Four cells showing firing dependent on location (corresponding to head direction) on the circle track, but not showing any modulation of firing rate dependent on head direction angle on the rotating pedestal. One of eight place cells had a bimodal tuning curve.

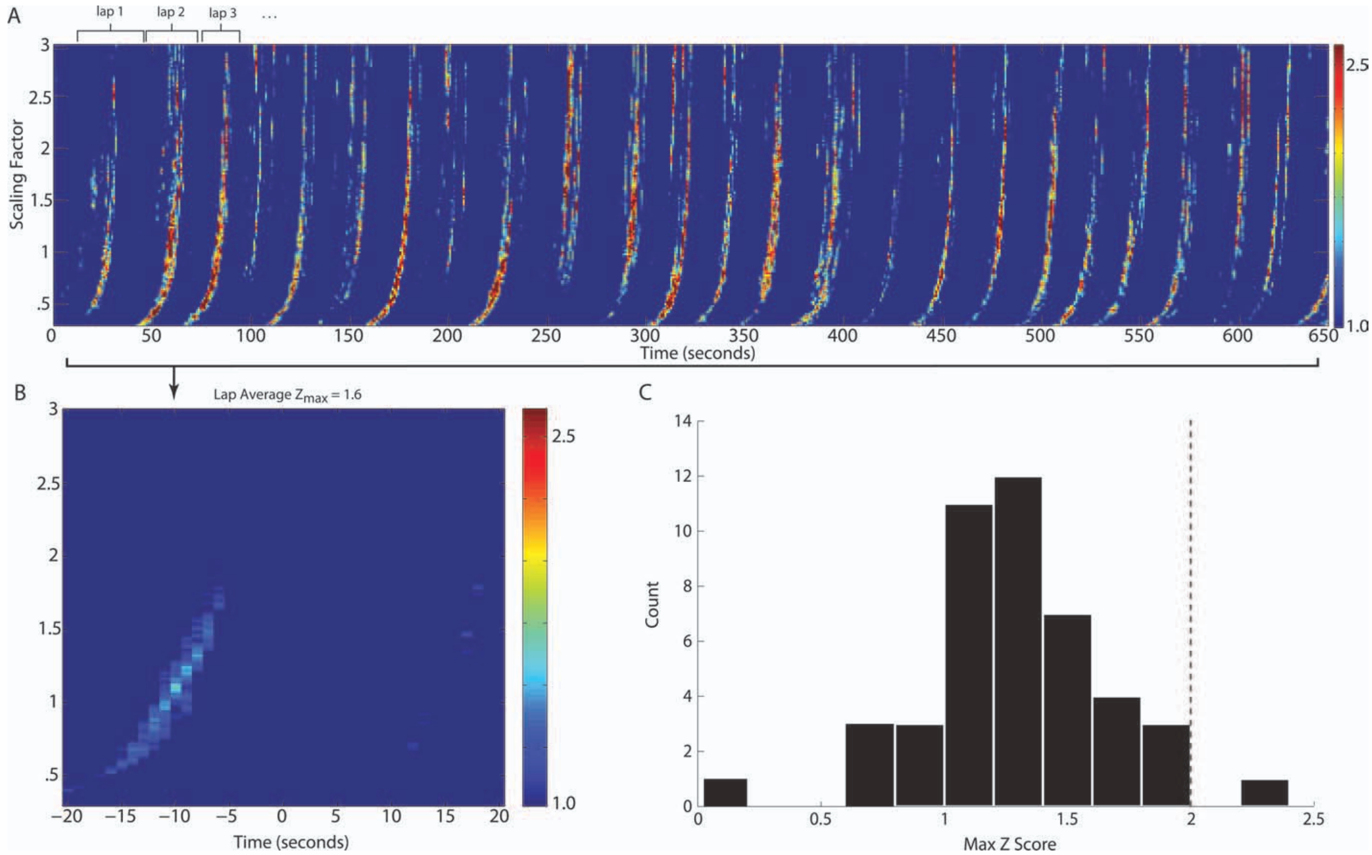

FIGURE 3. REM replay analysis. A: An example of the analysis output for correlation between one REM epoch and the entire RUN epoch. *Z* scores from the correlation (Ct) analysis are shown corresponding to specific times (in seconds) during running on the circular track (*x* axis) and corresponding to specific scaling factors on the *y* axis. The color at each point indicates the magnitude of the lowest *Z* score comparing the REM to RUN correlation with the shuffled data (see color scale bar in 3B). *Z* scores >2.0 indicate statistically similar replay activity for a given REM epoch. B: Lap average of *Z* scores. Laps were aligned according to the time that the rat crossed the south end of the circular track. C: Histogram showing the maximum *Z* score in the lap averaged data for each of 45 different REM epochs obtained from six different ensembles of neurons.

correlations between lap activity and REM activity (see Fig. 4D). We conclude that even when behavioral differences are accounted for in a template matching analysis that temporally structured replay does not appear at a statistically significant level in the spiking activity of postsubiculum ensembles.

Reconstruction of head direction from ensemble activity may provide evidence of replay of directional trajectories during sleep in the form of sweeps. Figure 5 shows the reconstruction of head direction during time running on the circular track (5A), REM sleep (5B), and SWS (5C), with average ensemble firing frequency below each figure. The raster of spiking activity during waking (5A) shows regular periods of spiking associated with activation of head direction cells at specific locations on the circle task. During SWS and REM sleep (5B and 5C), these neurons show similar overall activity levels, but without the regular patterns associated with task performance.

The most probable head direction during the task often aligns well with the observed head direction, as is shown in 5A, which reconstructs a portion of the task not used to generate the statistical model. When the Bayesian reconstruction algorithm was applied to ensemble activity during sleep, however, the most probable head direction jumped erratically. We saw no sweeps for either epoch during sleep, and there was a bias for the most probable head direction (about 100°, where the animal spends most of its time at the feeder), especially when average firing frequency was low. This effect was consistent across sessions, and consistent for sleep before and after the task. Figure 5D shows the probability of non-zero change in estimated head direction, sample to sample, for task, REM, and SWS during the session. A high probability for small changes in estimated head direction indicates coherent sweeps of activity during waking. From this it is clear that the task reconstruction favors clockwise rotations (arrow in Fig. 5D) indicating the running direction around the track and small changes in estimated head direction. The probability of large magnitude changes in estimated head direction for both REM and SWS is substantially higher than during task, indicating the lack of coherent sweeps of activity. Although the probability of change in estimated head direction is more uniform in both REM and SWS than task, there is still a peak for small magnitude changes in head direction because of the inherent bias towards the most probable head direction.

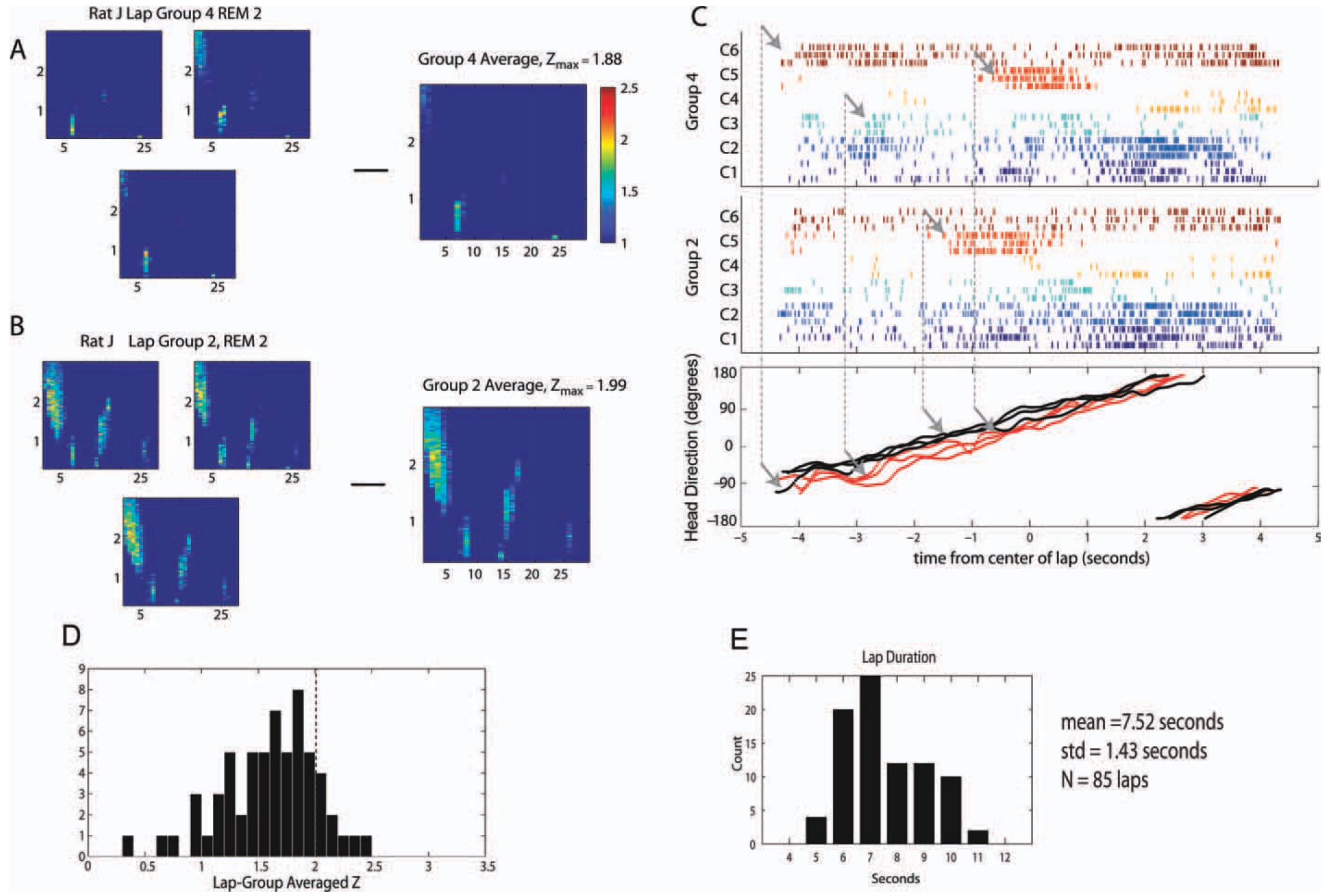

FIGURE 4. Modified REM replay analysis. We modified the original template analysis by Louie and Wilson (2001), so that each lap was its own template for comparison to every REM epoch. Thus, peaks in the resulting matrix of Z scores, Z (SF, t), will align if the laps are statistically similar to one another. To test for significance between laps, Z scores were computed pair-wise across all laps. A and B depict two groups of laps, which were significantly different from one another. This is clear from the position of the peaks in Z scores for the same REM epoch. In this analysis we only averaged those similar laps, so we did not destroy the peaks by averaging. C: Raster plots of head direction cells in both lap groups for each lap, and corresponding head direction. Every color denotes a unique head direction cell, whereas multiple rows are the independent laps within each group. Arrows indicate the difference in activity early in the lap, and shift in fields relative to one another within laps which correlate to different head direction positions between lap groups. Thus, the neuronal activity accurately reflects similarities and differences in behavior between laps. D: Histogram of peak Z scores for all REM epochs in all animals, as calculated by the modified REM replay analysis. Despite efforts to account for loss of significance by the effects of averaging, the number of significant peaks is still low. E: Lap statistics for novel analysis. The collected distribution of all lap duration shows one peak, but in two of four sessions there were two distinct peaks: one for slower laps and another for faster laps.

We were interested to address whether replay could occur in the postsubiculum during SWS, and specifically during sharp-wave-ripple events in the hippocampus. In our two animals, with EEG electrodes in the hippocampus, we were able to detect sharp wave ripples and look for activation of head direction cells and neurons responsive to place in the postsubiculum. Interestingly, we found that head direction cells were not affected by hippocampal ripples (see Fig. 6B) but the neurons responsive to place showed a strong activation during hippocampal ripples (see Fig. 6A). Figure 6C shows a significant difference in the probability of firing centered at hippocampal ripples between head direction cells and neurons responsive to place. The activation of cells responsive to place is significant at the center of the ripple as well as 40 ms after the center of the ripple, but not 40 ms before the ripple. We conclude that cells responsive to place but not cells responsive to head direction are activated during hippocampal ripples, and that the 40 ms delay in probability indicated a causal role for hippocampal ripples in eliciting activity of postsubicular place responsive cells, a possible mechanism in spatial memory formation.

DISCUSSION

These data addressed the question of whether head direction cells of the postsubiculum participate in hippocampal replay events during REM sleep and SWS sleep. The activity of large ensembles of head direction cell spiking data during REM sleep did not correlate strongly with activity observed on a repetitive circle task. In addition, during SWS individual head direction cells were rarely influenced by hippocampal sharp wave ripple events.

This data was aimed at testing potential circuit mechanics that could underlie retrieval in the medial temporal lobe memory system. Rodent unit studies have shown the replay of extended trajectories during REM sleep in region CA1 of the hippocampus (Louie and Wilson, 2001). This replay could be carried out within the hippocampus alone, or within a larger

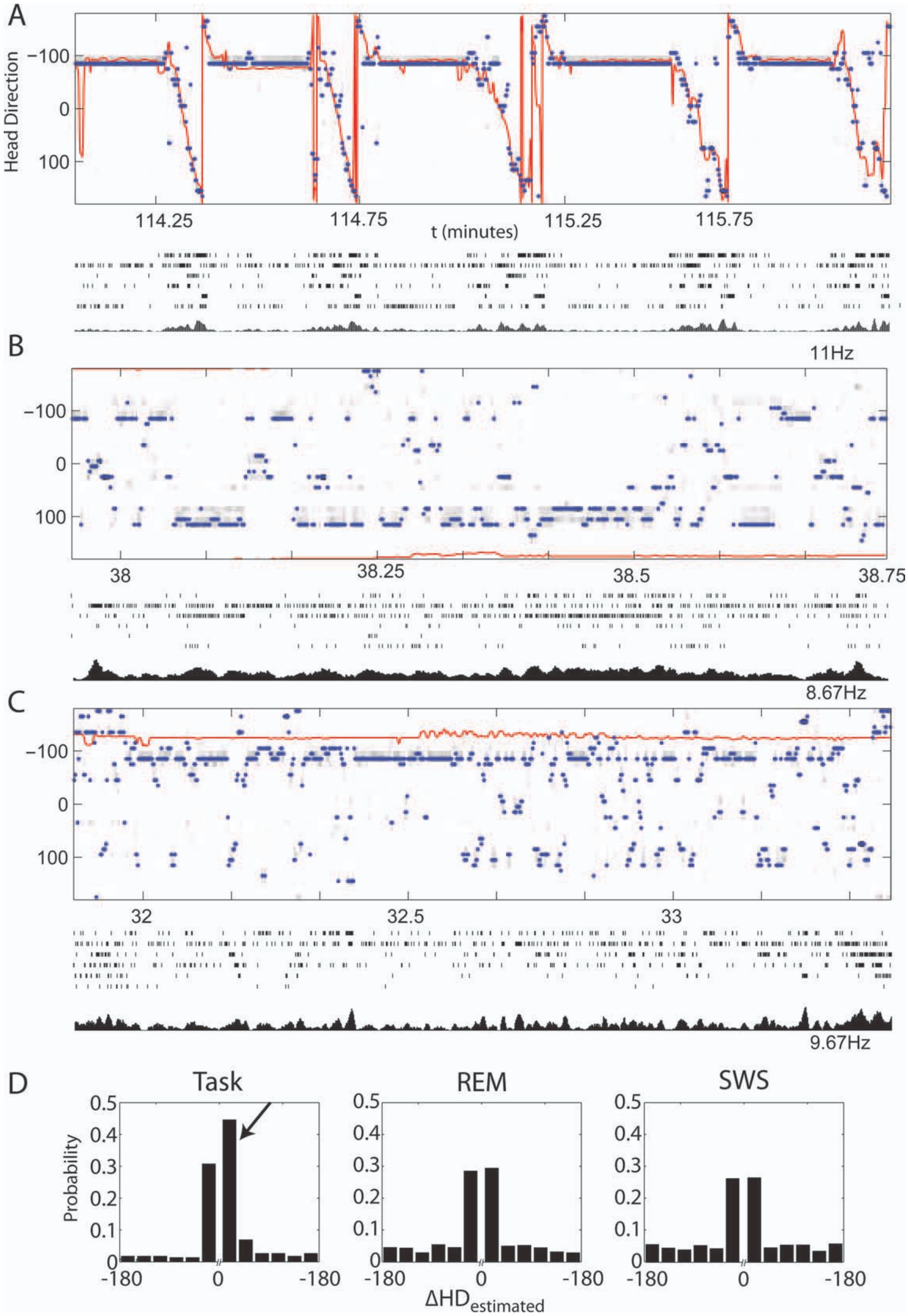

FIGURE 5.

circuit activated by replay processes (Hasselmo, 2008b; Hasselmo and Brandon, 2008). The study presented here investigated the possible involvement of the postsubiculum in extended trajectory retrieval by isolating multiple head direction cells during REM sleep and behavior on a repetitive circle track. Despite our ability to record many postsubiculum head direction cells simultaneously on our task, we did not observe a significant trajectory retrieval mediated by head direction cells during REM sleep.

In addition, we analyzed the activity of these cells during sharp-wave-ripple events in the hippocampus in SWS and report that these events do not elicit spiking in head direction cells, but do trigger increased spiking in postsubicular cells sensitive to place. Previous studies have shown that hippocampal ripples trigger spiking and replay in distant brain structures with a wide functionality, including the primary visual cortex (Ji and Wilson, 2007), ventral striatum (Pennartz et al., 2004), and prefrontal cortex (Euston et al., 2007). These observations indicate that ripple triggered replay is prominent in a variety of brain regions, and thus it is surprising that head direction cells in the postsubiculum, which has close connections with the hippocampus, do not participate in these coordinated ripple events.

Projections from region CA1 of the hippocampus to the dorsal presubiculum (postsubiculum) have been reported (van Groen and Wyss, 1990). This is not a strong pathway and has not been reported in some studies, but even if the direct projection is weak there are indirect projections from hippocampus to subiculum to postsubiculum (Naber and Witter, 1998) that allow an influence of region CA1 activity on head direction activity in postsubiculum. A recent model uses these connections to simulate REM replay (Hasselmo, 2008b; Hasselmo and Brandon, 2008). In this model, head direction cells drive grid cell activity during waking, and grid cell activity drives place cell activity. During awake behavior, coactive hippocampal place cells and postsubicular head direction cells become associated via synaptic modification. Then, during REM replay, the postsubiculum-entorhinal-hippocampal circuit replays the sequence of visited locations (Hasselmo, 2008b). Hippocampal place cells representing one location drive the associated head direction cells, which in turn shift the oscillation phase of a population of grid cells. These grids then drive the next group of hippocampal place cells representing the next location. Thus, this circuit can readout previously experienced spatiotemporal trajectories. This generated the hypothesis that replay of head direction activity during REM sleep or SWS could be associated with replay of head direction activity. The present results do not support an influence of place cells on head direction cells in the postsubiculum during REM replay. As an alternative, the model could use strengthening of connections between hippocampal place cells and head direction responsive cells in the deep layers of the entorhinal cortex (Sargolini et al., 2006).

Head Direction Cells Versus Neurons Responsive to Place

The data presented here do not support a role for postsubicular head direction cells in contributing to the REM sleep replay of spiking activity coding trajectories. However, these data do not rule out other circuit level mechanisms for the replay of previously encoded trajectories. In particular, the postsubiculum could still interact with the entorhinal cortex and hippocampus for replay of trajectories through involvement of place by head direction cells (Cacucci et al., 2004). Recent work has demonstrated that place responsive neurons in the postsubiculum are grid cells (Bocarra, 2010). We did not obtain sufficient numbers of simultaneously recorded neurons responsive to place in these studies to use the analytical techniques to analyze the role of place sensitive neurons in trajectory replay, but we did find that these neurons show significant spiking during ripples in contrast to cells that show pure head direction responses (Fig. 5). Thus, the possibility remains open for a replay circuit that involves postsubicular place by head direction cells (Cacucci et al., 2004). In fact, models of trajectory replay that perform Hebbian strengthening of connections between place cells and head direction cells (Hasselmo, 2008b, 2009; Hasselmo and Brandon, 2008) can simulate how the ac-

FIGURE 5. Decoded representation of head direction during waking and sleep. A: Bayesian reconstruction of head direction provides the probability of head direction *r* given neuron ensemble activity n, *P*(r|n) during active running on the circular track, without continuity constraint, shown in gray color map. Observed head direction, which was not included in generating the statistical model, is shown in red. Blue points indicate max[*P*(*r*|*n*)], which closely match the observed samples during the task. Below is the average firing frequency of ensemble neurons, and raster of ensemble spiking activity. Spiking of cells during the circular maze task is regular and associated with repeated activation of cells at specific locations on the track. There were five head direction cells and one place cell in this session. B: Reconstruction of head direction during REM given the model generated during task shown in A. Note that average firing frequency has decreased, and the decoded head direction jumps around erratically. The estimation also tends to return to the most likely head direction (from time spent at the feeder) at about -100°. Spiking of cells during REM does not show regular patterns correlated with prior task performance. C: Reconstruction of head direction during SWS also shows lack of coherent sweeps of activity, and tends to hover about the most probable head direction, especially when average firing rate falls close to zero. Spiking of cells during SWS does not show regular patterns correlated with prior task performance. D: Probability of change in head direction for task, REM, and SWS. Discontinuity in the *x* axis indicates that only non-zero changes in estimated head direction were included in the distribution. This was done to explore the coherency of potential "sweeps." Higher probability for small changes in estimated head direction indicate more coherent sweeps, since there was no continuity constraint. Task shows a bias for positive changes in head direction (indicated by arrow), which corresponds to the direction of running around the circular track. Task shows a much higher probability for smaller, more continuous changes in estimated head direction than either REM or SWS. The probabilities shown in REM and SWS are more uniform than task, but still prefer smaller changes in head direction because there is a preferred head direction component of the Bayesian decoding method.

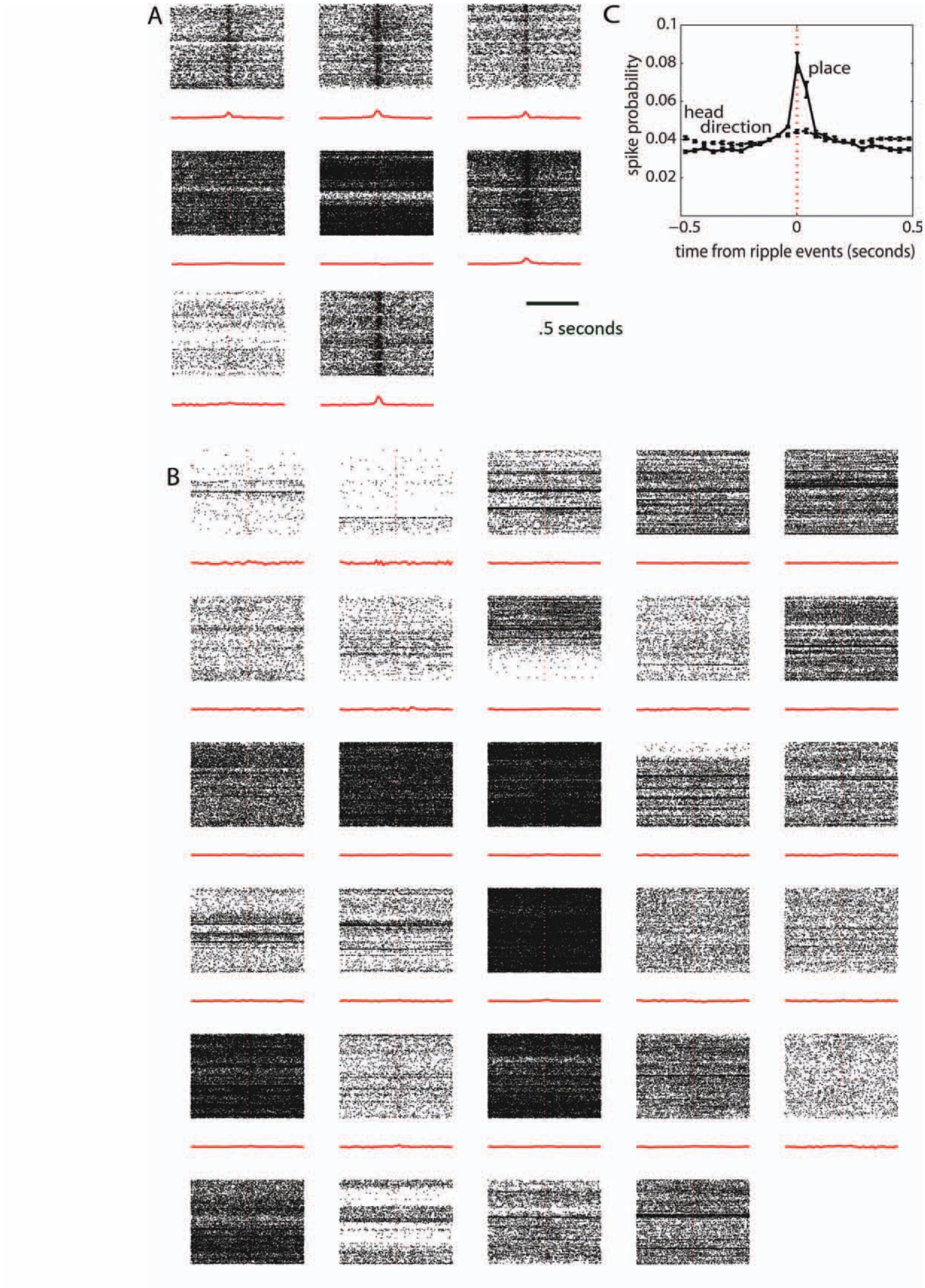

FIGURE 6. Ripple activation. A: Firing of neurons responsive to place around ripple events. Raster plots of action potentials 0.5 s before and 0.5 s after ripple centers shows activation in 5 of 8 neurons responsive to place. Histogram of firing is shown below, in red. For each cell, the cumulative spikes around all ripples during RUN were used. B: Firing of neurons responsive to head direction around ripple events. Note that no cells are activated at ripples. C: Average probability for each bin across cells. The probability distribution of firing was calculated by binning spikes in 40 ms bins from −0.5 to 0.5 s around each ripple event. Error bars indicate SEM. For place cells, $N = 8$ and for head direction cells, $N = 29$. [Color figure can be viewed in the online issue, which is available at wileyonlinelibrary.com.]

tivity of head direction cells could become increasingly similar to place by head direction cells. However, the input to postsubiculum from other regions such as anterior thalamus and retrosplenial cortex, and the time spent in other environments could prevent a growing influence of place on head direction cells.

Hippocampal-Entorhinal Circuitry Could Support Trajectory Retrieval

The combined evidence that trajectory retrieval occurs during REM in the hippocampus (Louie and Wilson, 2001) but not in head direction cells in the postsubiculum suggests that hippocampal-entorhinal circuitry alone might support replay during REM. Entorhinal cortical neurons in layer II project to the dentate gyrus and region CA3 of the hippocampus, and entorhinal layer III neurons project to region CA1 (Witter et al., 2000; Canto et al., 2008). Region CA1 neurons connect back to deep layers of the same area of entorhinal cortex either directly or via the subiculum (Tamamaki and Nojyo, 1995; Witter et al., 2000). These deep layers then project to the corresponding area in superficial entorhinal layers, completing a potential loop for mediating replay. Head direction cells are abundant within deep layers of the medial entorhinal cortex (Sargolini et al., 2006) and have wider tuning curves than postsubiculum head direction cells (Taube et al., 1990a; Sargolini et al., 2006). The wide tuning seen in medial entorhinal head direction cells could reflect greater plasticity that has occurred with head direction cells with adjacent tuning curves or with afferents from region CA1 or the subiculum. Future trajectory replay models and experiments should focus on medial entorhinal layer V cells as a potential site for formation of associations between place cells and head direction activity and replay of sequences observed during waking.

The Postsubiculum as an Afferent Input to Grid Cells

The data presented here are consistent with head direction cells in the postsubiculum selectively coding the veridical heading of an animal in the environment without influences of prior memory. As shown by extensive prior research (Taube et al., 1990a,b; Blair and Sharp, 1995; Taube and Burton, 1995; Taube, 1995; Blair and Sharp, 1996; Sharp, 1996; Blair et al., 1997; Goodridge and Taube, 1997; Stackman and Taube, 1997; Blair et al., 1998; Stackman and Taube, 1998; Taube, 1998; Stackman et al., 2000; Sharp et al., 2001; Stackman et al., 2003; Taube and Bassett, 2003; Taube, 2004; Johnson et al., 2005; Yu et al., 2006), the head direction cell system constitutes an independent pathway using vestibular input to provide spatial heading information to the medial entorhinal cortex and hippocampus. Work by Taube has traced many stages of the pathway from the vestibular nuclei to the postsubiculum (Taube and Bassett, 2003), which includes head direction cells in the brain stem, the lateral mammillary nucleus (Blair et al., 1998; Stackman and Taube, 1998), the anterior thalamus (Taube, 1995; Stackman and Taube, 1997), the postsubiculum (Taube et al., 1990a,b; Johnson et al., 2005), and the medial entorhinal cortex (Sargolini et al., 2006). Head direction firing in the anterior thalamus is blocked by lesions of vestibular input (Stackman and Taube, 1997) and depends on voluntary movement (Taube, 1995), indicating the direct role of sensory update. In the postsubiculum the head direction firing incorporates the influence of visual stimuli, following visual cue cards and persisting without voluntary movement (Goodridge and Taube, 1997; Taube and Bassett, 2003). These data indicate that the head direction signal could provide an accurate self-motion signal based on sensory input to update spatial representations in the medial entorhinal cortex. The head direction signal input to the medial entorhinal cortex has been proposed to generate the spatial representations provided by grid cells of medial entorhinal cortex in both oscillatory interference models (Burgess et al., 2007; Giocomo et al., 2007; Burgess, 2008; Hasselmo, 2008a) as well as attractor dynamic models (Fuhs and Touretzky, 2006; McNaughton et al., 2006; Burak and Fiete, 2009). Alternately, the head direction signal could interact with speed modulated rhythmic inhibition to shift the phase of resonant activity. Several models have illustrated how place cell responses could be generated via grid cell synaptic inputs onto hippocampal neurons (Rolls et al., 2006; Solstad et al., 2006; Hasselmo, 2008b; de Almeida et al., 2009). Thus, head direction cells could provide the input that generates both grid cells and place cells, but our data suggests that they may not be involved in the reactivation of place cells during REM sleep. Taken with the observation that head direction cells do not "remap" with respect to each other, our data suggests the possibility that the postsubiculum head direction network does not participate in all the dynamics of the hippocampal place cell network.

REFERENCES

Blair HT, Lipscomb BW, Sharp PE. 1997. Anticipatory time intervals of head-direction cells in the anterior thalamus of the rat: Implications for path integration in the head-direction circuit. J Neurophysiol 78:145–159.

Blair HT, Cho J, Sharp PE. 1998. Role of the lateral mammillary nucleus in the rat head direction circuit: A combined single unit recording and lesion study. Neuron 21:1387–1397.

Blair HT, Sharp PE. 1995. Anticipatory head direction signals in anterior thalamus: Evidence for a thalamocortical circuit that integrates angular head motion to compute head direction. J Neurosci 15:6260–6270.

Blair HT, Sharp PE. 1996. Visual and vestibular influences on head-direction cells in the anterior thalamus of the rat. Behav Neurosci 110:643–660.

Boccara CN, Sargolini F, Thoresen VH, Solstad T, Witter MP, Moser EI, Moser MB. 2010. Grid cells in pre- and parasubiculum. Nat Neurosci 13:987–994.

Burak Y, Fiete IR. 2009. Accurate path integration in continuous attractor network models of grid cells. PLoS Comput Biol 5:e1000291.

Burgess N. 2008. Grid cells and theta as oscillatory interference: Theory and predictions. Hippocampus 18:1157–1174.

Burgess N, Barry C, O'Keefe J. 2007. An oscillatory interference model of grid cell firing. Hippocampus 17:801–812.
Buzsaki G. 1989. Two-stage model of memory trace formation: A role for "noisy" brain states. Neuroscience 31:551–570.
Cacucci F, Lever C, Wills TJ, Burgess N, O'Keefe J. 2004. Theta-modulated place-by-direction cells in the hippocampal formation in the rat. J Neurosci 24:8265–8277.
Canto CB, Wouterlood FG, Witter MP. 2008. What does the anatomical organization of the entorhinal cortex tell us? Neural Plast 2008:381243.
Davidson TJ, Kloosterman F, Wilson MA. 2009. Hippocampal replay of extended experience. Neuron 63:497–507.
de Almeida L, Idiart M, Lisman JE. 2009. The input-output transformation of the hippocampal granule cells: From grid cells to place fields. J Neurosci 29:7504–7512.
Diba K, Buzsaki G. 2007. Forward and reverse hippocampal place-cell sequences during ripples. Nat Neurosci 10:1241–1242.
Euston DR, Tatsuno M, McNaughton BL. 2007. Fast-forward playback of recent memory sequences in prefrontal cortex during sleep. Science 318:1147–1150.
Foster DJ, Wilson MA. 2006. Reverse replay of behavioral sequences in hippocampal place cells during the awake state. Nature 440:680–683.
Fuhs MC, Touretzky DS. 2006. A spin glass model of path integration in rat medial entorhinal cortex. J Neurosci 26:4266–4276.
Gaile GL, Burt JE. 1980. Directional Statistics, Concept and Techniques in Modern Geography, No 25. Norwich, England: Geo Abstracts Ltd. pp 10–14.
Giocomo LM, Zilli EA, Fransen E, Hasselmo ME. 2007. Temporal frequency of subthreshold oscillations scales with entorhinal grid cell field spacing. Science 315:1719–1722.
Goodridge JP, Taube JS. 1997. Interaction between the postsubiculum and anterior thalamus in the generation of head direction cell activity. J Neurosci 17:9315–9330.
Hafting T, Fyhn M, Molden S, Moser MB, Moser EI. 2005. Microstructure of a spatial map in the entorhinal cortex. Nature 436:801–806.
Hasselmo ME. 2008a. Grid cell mechanisms and function: Contributions of entorhinal persistent spiking and phase resetting. Hippocampus 18:1213–1229.
Hasselmo ME. 2008b. Temporally structured replay of neural activity in a model of entorhinal cortex, hippocampus and postsubiculum. Eur J Neurosci 28:1301–1315.
Hasselmo ME. 2009. A model of episodic memory: Mental time travel along encoded trajectories using grid cells. Neurobiol Learn Mem 92:559–573.
Hasselmo ME, Brandon MP. 2008. Linking cellular mechanisms to behavior: Entorhinal persistent spiking and membrane potential oscillations may underlie path integration, grid cell firing, and episodic memory. Neural Plast 2008:658323.
Hasselmo ME, Wyble BP, Wallenstein GV. 1996. Encoding and retrieval of episodic memories: Role of cholinergic and GABAergic modulation in the hippocampus. Hippocampus 6:693–708.
Ji D, Wilson MA. 2007. Coordinated memory replay in the visual cortex and hippocampus during sleep. Nat Neurosci 10: 100–107.
Johnson A, Seeland K, Redish AD. 2005. Reconstruction of the postsubiculum head direction signal from neural ensembles. Hippocampus 15:86–96.
Karlsson MP, Frank LM. 2009. Awake replay of remote experiences in the hippocampus. Nat Neurosci 12:913–918.
Knierim JJ, Kudrimoti HS, McNaughton BL. 1995. Place cells, head direction cells, and the learning of landmark stability. J Neurosci 15:1648–1659.
Lee AK, Wilson MA. 2002. Memory of sequential experience in the hippocampus during slow wave sleep. Neuron 36:1183–1194.
Louie K, Wilson MA. 2001. Temporally structured replay of awake hippocampal ensemble activity during rapid eye movement sleep. Neuron 29:145–156.
McClelland JL, McNaughton BL, O'Reilly RC. 1995. Why there are complementary learning systems in the hippocampus and neocortex: Insights from the successes and failures of connectionist models of learning and memory. Psychol Rev 102:419–457.
McNaughton BL, Barnes CA, O'Keefe J. 1983. The contributions of position, direction, and velocity to single unit-activity in the hippocampus of freely-moving rats. Exp Brain Res 52:41–49.
McNaughton BL, Battaglia FP, Jensen O, Moser EI, Moser MB. 2006. Path integration and the neural basis of the cognitive map. Nat Rev Neurosci 7:663–678.
Morris RG, Garrud P, Rawlins JN, O'Keefe J. 1982. Place navigation impaired in rats with hippocampal lesions. Nature 297:681–683.
Moser EI, Moser MB. 2008. A metric for space. Hippocampus 18:1142–1156.
Muller RU, Kubie JL, Ranck JB Jr. 1987. Spatial firing patterns of hippocampal complex-spike cells in a fixed environment. J Neurosci 7:1935–1950.
Naber PA, Witter MP. 1998. Subicular efferents are organized mostly as parallel projections: A double-labeling, retrograde-tracing study in the rat. J Comp Neurol 393:284–297.
Nguyen DP, Wilson MA, Brown EN, Barbieri R. 2009. Measuring instantaneous frequency of local field potential oscillations using the Kalman smoother. J Neurosci Methods 184:365–374.
O'Keefe J, Dostrovsky J. 1971. The hippocampus as a spatial map. Preliminary evidence from unit activity in the freely-moving rat. Brain Res 34:171–175.
Pennartz CM, Lee E, Verheul J, Lipa P, Barnes CA, McNaughton BL. 2004. The ventral striatum in off-line processing: Ensemble reactivation during sleep and modulation by hippocampal ripples. J Neurosci 24:6446–6456.
Rolls ET, Stringer SM, Elliot T. 2006. Entorhinal cortex grid cells can map to hippocampal place cells by competitive learning. Network 17:447–465.
Sargolini F, Fyhn M, Hafting T, McNaughton BL, Witter MP, Moser MB, Moser EI. 2006. Conjunctive representation of position, direction, and velocity in entorhinal cortex. Science 312:758–762.
Sharp PE. 1996. Multiple spatial/behavioral correlates for cells in the rat postsubiculum: Multiple regression analysis and comparison to other hippocampal areas. Cereb Cortex 6:238–259.
Sharp PE, Blair HT, Cho J. 2001. The anatomical and computational basis of the rat head-direction cell signal. Trends Neurosci 24:289–294.
Skaggs WE, McNaughton BL. 1996. Replay of neuronal firing sequences in rat hippocampus during sleep following spatial experience. Science 271:1870–1873.
Solstad T, Moser EI, Einevoll GT. 2006. From grid cells to place cells: A mathematical model. Hippocampus 16:1026–1031.
Stackman RW, Taube JS. 1997. Firing properties of head direction cells in the rat anterior thalamic nucleus: Dependence on vestibular input. J Neurosci 17:4349–4358.
Stackman RW, Taube JS. 1998. Firing properties of rat lateral mammillary single units: Head direction, head pitch, and angular head velocity. J Neurosci 18:9020–9037.
Stackman RW, Tullman ML, Taube JS. 2000. Maintenance of rat head direction cell firing during locomotion in the vertical plane. J Neurophysiol 83:393–405.
Stackman RW, Golob EJ, Bassett JP, Taube JS. 2003. Passive transport disrupts directional path integration by rat head direction cells. J Neurophysiol 90:2862–2874.
Steffenach HA, Witter M, Moser MB, Moser EI. 2005. Spatial memory in the rat requires the dorsolateral band of the entorhinal cortex. Neuron 45:301–313.
Tamamaki N, Nojyo Y. 1995. Preservation of topography in the connections between the subiculum, field CA1, and the entorhinal cortex in rats. J Comp Neurol 353:379–390.

Taube JS. 1995. Head direction cells recorded in the anterior thalamic nuclei of freely moving rats. J Neurosci 15 (1 Part 1):70–86.
Taube JS. 1998. Head direction cells and the neurophysiological basis for a sense of direction. Prog Neurobiol 55:225–256.
Taube JS. 2004. Interspike interval analyses on anterior dorsal thalamic head direction cells. Soc Neurosci Abstr 30:868.12.
Taube JS, Bassett JP. 2003. Persistent neural activity in head direction cells. Cereb Cortex 13:1162–1172.
Taube JS, Burton HL. 1995. Head direction cell activity monitored in a novel environment and during a cue conflict situation. J Neurophysiol 74:1953–1971.
Taube JS, Muller RU, Ranck JB Jr. 1990a. Head-direction cells recorded from the postsubiculum in freely moving rats. I. Description and quantitative analysis. J Neurosci 10:420–435.
Taube JS, Muller RU, Ranck JB Jr. 1990b. Head-direction cells recorded from the postsubiculum in freely moving rats. II. Effects of environmental manipulations. J Neurosci 10:436–447.
Taube JS, Kesslak JP, Cotman CW. 1992. Lesions of the rat postsubiculum impair performance on spatial tasks. Behav Neural Biol 57:131–143.
van Groen T, Wyss JM. 1990. The postsubicular cortex in the rat: Characterization of the fourth region of the subicular cortex and its connections. Brain Res 529:165–177.
Wilson MA, McNaughton BL. 1994. Reactivation of hippocampal ensemble memories during sleep. Science 265:676–679.
Witter MP, Wouterlood FG, Naber PA, Van Haeften T. 2000. Anatomical organization of the parahippocampal-hippocampal network. Ann N Y Acad Sci 911:1–24.
Wood ER, Dudchenko PA, Robitsek RJ, Eichenbaum H. 2000. Hippocampal neurons encode information about different types of memory episodes occurring in the same location. Neuron 27:623–633.
Yu X, Yoganarasimha D, Knierim JJ. 2006. Backward shift of head direction tuning curves of the anterior thalamus: Comparison with CA1 place fields. Neuron 52:717–729.